Modeling elastic wave forward propagation and reflection using the complex screen method

Xiao-Bi Xie and Ru-Shan Wu
Institute of Geophysics and Planetary Physics, University of California, Santa Cruz, California 95064

(Received 18 January 2000; revised 24 February 2001; accepted 27 February 2001)

Formulation for calculating forward propagation and reflection in a 3D elastic structure based on the complex-screen method is given in this paper. The calculation of reflections is formulated based on the local Born approximation. When using a small angle approximation, the backscattering operator reduces to a screen operator which is similar to the forward screen propagator. Combining the forward propagator and backscattering operator together, the new method can properly handle the multiple forward scattering and single backscattering in a 3D heterogeneous model. Using a dual-domain technique, the new method is highly efficient in CPU time and memory savings. For models where reverberation and resonance scattering can be neglected, this method provides a fast and accurate algorithm. Synthetic seismograms for two-dimensional elastic models are calculated with this method and compared with those generated by the finite-difference method. The results show that the method works well for small to medium scattering angles and medium velocity contrasts. © *2001 Acoustical Society of America.* [DOI: 10.1121/1.1367248]

PACS numbers: 43.20.Gp, 43.20.Bi [ANN]

I. INTRODUCTION

Fast modeling methods and algorithms in complex heterogeneous media, especially for 3D media, are crucial to the application of seismic methods in complex structures including the development of interpretation, imaging and inversion methods. Finite-difference and finite-element algorithms are very flexible. In principle, they can be applied to arbitrarily heterogeneous medium. However, they are very time consuming. High-frequency asymptotic methods, such as ray based methods (e.g., Červený, 1981; Červený and Klimes, 1984; Chapman, 1985), provide high computation efficiency for smooth 3D models. However, they fail to deal with complicated 3D volume heterogeneities. Frequency-dependent and wave related phenomena in complex media cannot be correctly modeled by the ray methods. Born scattering formulation (Gubernatis *et al.*, 1977; Wu and Aki, 1985), ray-Born (Beydoun and Mendes, 1989; Coates and Chapman, 1990), or generalized Born scattering methods (Coates and Chapman, 1991) can model small volume complex heterogeneities in a smooth background. However, they are not capable of modeling long distance propagation in complex media. It is necessary to develop intermediate modeling methods functioning between the full wave equation methods and the high-frequency asymptotic methods.

The phase screen method, or split step Fourier method (e.g., Flatté and Tappert, 1975; Tappert, 1977; Thomson and Chapman, 1983), has been used to calculate the one-way forward propagation for acoustic waves. Recently, the method has also been used to deal with elastic waves. To generalize a scalar wave case to vector elastic waves, the center part is the coupling between *P*- and *S*-waves. Fisk and McCartor (1991) derived coupling terms using a projection method. Their method has some problems for some limiting cases. Wu (1994) derived these terms based on formal scattering theory of elastic waves. Wild and Hudson (1998) used another approach, the geometrical derivation, and reached similar results. The screen method has also been used as back propagators for seismic wave migration in either acoustic or elastic media (e.g., Stoffa *et al.*, 1990; Wu and Xie, 1994; Huang *et al.*, 1999). Generally speaking, these methods give better imaging quality compared with the ray based Kirchhoff method. The generalized screen methods are based on the one-way wave equation that neglects backscattered waves, but correctly handles all the forward multiple-scattering effects, e.g., focusing/defocusing, diffraction, interference, and conversion between different wave types. For media where the resonance scattering or reverberations caused by heterogeneities can be neglected, the reflections will be dominated by single backscatterings. In this case, the screen method can also be adopted to calculate reflections. Wu and Huang (1995) tested the method for acoustic reflections. Wu (1996) discussed approximations for forward and backward scatterings of different wave types. Xie and Wu (1996) tested the screen approximation for modeling elastic wave reflections.

In this study, the complex-screen method is extended to deal with both forward propagation and reflection of elastic waves. The current formulation is based on a small angle approximation of the one-way wave equation and the local Born approximation using the perturbation theory. Under the small angle approximation, backscattering can also be formulated into a screen operator which is similar to the screen propagator. The interaction between the incident wave field and the heterogeneities gives both forward and backward scattered waves. The forward scattered waves, together with the primary wave, construct the transmitted waves. The backscattered waves give the reflections by the structure. With an iterative method, it can correctly handle multiple forward scattering and single backscattering. By using a dual-domain operation, it retains the advantages of the original screen method, i.e., high-efficiency in computation speed and tremendous memory savings. Numerical results show that this is a very promising method in modeling primary reflections from complicated large scale 3D elastic structures.

In the following sections, we first present the formulation. Then numerical examples are conducted to test the method. For a two-dimensional test model, the results from the screen method are compared with that from the full wave finite-difference method.

II. EXPRESSIONS FOR FORWARD AND BACKWARD SCATTERED WAVE FIELDS

We start from the equation of motion for displacement $\mathbf{u}$ in a linear elastic medium (Aki and Richards, 1980):

$$-\rho(\mathbf{x})\omega^2\mathbf{u}(\mathbf{x})=\nabla\cdot[\tfrac{1}{2}\mathbf{c}(\mathbf{x}):(\nabla\mathbf{u}(\mathbf{x})+\mathbf{u}(\mathbf{x})\nabla)], \tag{1}$$

where $\mathbf{u}$ is the displacement, $\mathbf{c}$ is the elastic constant tensor, ρ is density, $\mathbf{u}\nabla$ is the transpose of $\nabla\mathbf{u}$ and ‘‘:’’ is for double scalar product, i.e., $(\mathbf{ab}):(\mathbf{cd})=(\mathbf{b}\cdot\mathbf{c})(\mathbf{a}\cdot\mathbf{d})$. If elastic parameters and the wave field can be decomposed into

$$\rho(\mathbf{x})=\rho_0+\delta\rho(\mathbf{x}),$$
$$\mathbf{c}(\mathbf{x})=\mathbf{c}_0+\delta\mathbf{c}(\mathbf{x}),$$
$$\mathbf{u}(\mathbf{x})=\mathbf{u}_0(\mathbf{x})+\mathbf{U}(\mathbf{x}),$$

where ρ_0 and $\mathbf{c}_0$ are density and elastic parameters for the background medium, $\delta\rho(\mathbf{x})$ and $\delta\mathbf{c}(\mathbf{x})$ are the corresponding perturbations, $\mathbf{u}_0(\mathbf{x})$ and $\mathbf{U}(\mathbf{x})$ are the incident field and the scattered field, then Eq. (1) can be rewritten as

$$-\rho_0\omega^2\mathbf{U}(\mathbf{x})-\nabla\cdot[\tfrac{1}{2}\mathbf{c}_0:(\nabla\mathbf{U}(\mathbf{x})+\mathbf{U}(\mathbf{x})\nabla)]=\mathbf{F}(\mathbf{x}), \tag{2}$$

where

$$\mathbf{F}(\mathbf{x})=\omega^2\delta\mathbf{c}(\mathbf{x})\mathbf{u}(\mathbf{x})+\nabla\cdot[\tfrac{1}{2}\delta\mathbf{c}(\mathbf{x}):(\nabla\mathbf{u}(\mathbf{x})+\mathbf{u}(\mathbf{x})\nabla)] \tag{3}$$

is the equivalent body force due to scattering. The scattered field can be expressed as

$$\mathbf{U}(\mathbf{x})=\int_{V'}dv'\,\mathbf{G}(\mathbf{x};\mathbf{x}')\mathbf{F}(\mathbf{x}'), \tag{4}$$

where $\mathbf{G}$ is the Green's function in the background medium. We will consider a special case where an incident wave $\mathbf{u}_0(\mathbf{x})$ interacts with a heterogeneous thin slab which is perpendicular to the main propagation direction. Figure 1 shows the primary incident waves and various types of secondary waves generated by the scattering process. If the slab is thin enough, the local Born approximation can be adopted within the slab. The wave field $\mathbf{u}(\mathbf{x})$ in Eq. (3) can be replaced by the incident field $\mathbf{u}_0(\mathbf{x})$. Let $\hat{\mathbf{e}}_z$ be the unit vector along the main propagation direction, and $\mathbf{x}_T=x\hat{\mathbf{e}}_x+y\hat{\mathbf{e}}_y$ be a position vector in the transverse plane. The slab is between z_0 and z_1, with a thickness of $\Delta z=z_1-z_0$. The scattered field from the slab can be expressed as

$$\mathbf{U}(\mathbf{x})=\int_{z_0}^{z_1}dz'\int\int d\mathbf{x}'_T\mathbf{G}(\mathbf{x}_T,z;\mathbf{x}'_T,z')\mathbf{F}_0(\mathbf{x}'_T,z'), \tag{5}$$

where $\mathbf{F}_0(\mathbf{x})$ is Eq. (3) with $\mathbf{u}(\mathbf{x})$ replaced by $\mathbf{u}_0(\mathbf{x})$.

The incident field $\mathbf{u}_0(\mathbf{x})$ can be decomposed into a superposition of plane P- and S-waves:

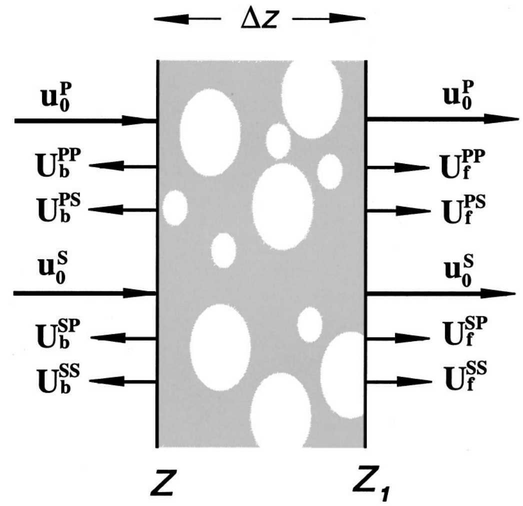

FIG. 1. A sketch showing the primary waves and various scattering waves generated when an incident wave interacts with an inhomogeneous thin slab. For details see text.

$$\mathbf{u}_0(\mathbf{x}_T,z)=\frac{1}{4\pi^2}\int d\mathbf{K}_T[\mathbf{u}_0^P(\mathbf{K}_T,z)+\mathbf{u}_0^S(\mathbf{K}_T,z)]e^{i\mathbf{K}_T\cdot\mathbf{x}_T}, \tag{6}$$

where $\mathbf{K}_T$ is the incident transverse wave number of plane waves and superscripts P and S denote P- and S-waves. The forward propagated field is composed of primary wave and forward scattered P- and S-waves. At z_1, it can be expressed as

$$\mathbf{u}_f(\mathbf{x}_T,z_1)=\frac{1}{4\pi^2}\int d\mathbf{K}'_T[\mathbf{u}_f^P(\mathbf{K}'_T,z_1)+\mathbf{u}_f^S(\mathbf{K}'_T,z_1)]e^{i\mathbf{K}'_T\cdot\mathbf{x}_T}, \tag{7}$$

where

$$\mathbf{u}_f^P(\mathbf{K}'_T,z_1)=e^{i\gamma'_\alpha|z_1-z_0|}[\mathbf{u}_0^P(\mathbf{K}'_T,z_0)+\mathbf{U}_f^{PP}(\mathbf{K}'_T,z_0)+\mathbf{U}_f^{SP}(\mathbf{K}'_T,z_0)], \tag{8}$$

$$\mathbf{u}_f^S(\mathbf{K}'_T,z_1)=e^{i\gamma'_\beta|z_1-z_0|}[\mathbf{u}_0^S(\mathbf{K}'_T,z_0)+\mathbf{U}_f^{SS}(\mathbf{K}'_T,z_0)+\mathbf{U}_f^{PS}(\mathbf{K}'_T,z_0)], \tag{9}$$

where $\mathbf{K}'_T$ is the transverse wave number of scattered waves, $\gamma_\alpha=(k_\alpha^2-K_T^2)^{1/2}$ and $\gamma_\beta=(k_\beta^2-K_T^2)^{1/2}$ are longitudinal components of P- and S-wave numbers in the background media, and $k_\alpha=\omega/\alpha$ and $k_\beta=\omega/\beta$ are P- and S-wave numbers, α and β are P- and S-wave velocities. Phase advance operators $e^{i\gamma'_\alpha|z_1-z_0|}$ and $e^{i\gamma'_\beta|z_1-z_0|}$ propagate the incident and scattered fields from z_0 to z_1. The reflected wave is composed of backscattered P- and S-waves. At z_0, the reflected wave can be expressed as

$$\mathbf{u}_b(\mathbf{x}_T,z_0)=\frac{1}{4\pi^2}\int d\mathbf{K}'_T[\mathbf{u}_b^P(\mathbf{K}'_T,z_0)+\mathbf{u}_b^S(\mathbf{K}'_T,z_0)]e^{i\mathbf{K}'_T\cdot\mathbf{x}_T}, \tag{10}$$

where

$$\mathbf{u}_b^P(\mathbf{K}'_T,z_0)=\mathbf{U}_b^{PP}(\mathbf{K}'_T,z_0)+\mathbf{U}_b^{SP}(\mathbf{K}'_T,z_0), \tag{11}$$

$$\mathbf{u}_b^S(\mathbf{K}_T',z_0)=\mathbf{U}_b^{PS}(\mathbf{K}_T',z_0)+\mathbf{U}_b^{SS}(\mathbf{K}_T',z_0). \tag{12}$$

In above equations, $\mathbf{U}$ denotes scattered waves. The subscripts f and b denote forward and backward scatterings, respectively. Superscripts *PP*, *PS*, *SP* and *SS* indicate the scattering between different wave types as shown in Fig. 1. For isotropic elastic medium, the scattered fields for both forward and backward scatterings can be derived from Eq. (5) (Wu, 1994):

$$\mathbf{U}^{PP}(\mathbf{K}_T',\mathbf{K}_T)=\frac{i}{2\gamma_\alpha'}k_\alpha^2 u_0^P \hat{k}_\alpha' \left\{ (\hat{k}_\alpha\cdot\hat{k}_\alpha')\frac{\delta\rho(\tilde{\mathbf{k}})}{\rho_0} - \frac{\delta\lambda(\tilde{\mathbf{k}})}{\lambda_0+2\mu_0} - (\hat{k}_\alpha\cdot\hat{k}_\alpha')^2 \frac{2\delta\mu(\tilde{\mathbf{k}})}{\lambda_0+2\mu_0}\right\}, \tag{13}$$

$$\mathbf{U}^{PS}(\mathbf{K}_T',\mathbf{K}_T)=\frac{i}{2\gamma_\beta'}k_\beta^2 u_0^P [\hat{k}_\alpha-\hat{k}_\beta'(\hat{k}_\alpha\cdot\hat{k}_\beta')] \left\{ \frac{\delta\rho(\tilde{\mathbf{k}})}{\rho_0} - 2\frac{\beta_0}{\alpha_0}(\hat{k}_\alpha\cdot\hat{k}_\beta')\frac{\delta\mu(\tilde{\mathbf{k}})}{\mu_0}\right\}, \tag{14}$$

$$\mathbf{U}^{SP}(\mathbf{K}_T',\mathbf{K}_T)=\frac{i}{2\gamma_\alpha'}k_\alpha^2 (\mathbf{u}_0^S\cdot\hat{k}_\alpha')\hat{k}_\alpha' \left\{ \frac{\delta\rho(\tilde{\mathbf{k}})}{\rho_0} - 2\frac{\beta_0}{\alpha_0}(\hat{k}_\beta\cdot\hat{k}_\alpha')\frac{\delta\mu(\tilde{\mathbf{k}})}{\mu_0}\right\}, \tag{15}$$

$$\begin{aligned}\mathbf{U}^{SS}(\mathbf{K}_T',\mathbf{K}_T)=\frac{i}{2\gamma_\beta'}k_\beta^2 \Bigg\{ & [\mathbf{u}_0^S-\hat{k}_\beta'(\mathbf{u}_0^S\cdot\hat{k}_\beta')]\frac{\delta\rho(\tilde{\mathbf{k}})}{\rho_0} \\ & -[(\hat{k}_\beta\cdot\hat{k}_\beta')[\mathbf{u}_0^S-\hat{k}_\beta'(\mathbf{u}_0^S\cdot\hat{k}_\beta')]+(\mathbf{u}_0^S\cdot\hat{k}_\alpha') \\ & \times(\hat{k}_\beta-\hat{k}_\beta'(\hat{k}_\beta\cdot\hat{k}_\beta'))]\frac{\delta\mu(\tilde{\mathbf{k}})}{\mu_0}\Bigg\},\end{aligned} \tag{16}$$

where $u_0^P=|\mathbf{u}_0^P(\mathbf{K}_T)|$ and $\mathbf{u}_0^S=\mathbf{u}_0^S(\mathbf{K}_T)$, $\delta\rho(\mathbf{k})$, $\delta\lambda(\mathbf{k})$ and $\delta\mu(\mathbf{k})$ are three-dimensional Fourier transforms of medium perturbations, wave numbers without primes are for incident waves and with primes are for scattered waves, $\tilde{\mathbf{k}}=\mathbf{k}'-\mathbf{k}$ is the exchange wave number with $\mathbf{k}$ and $\mathbf{k}'$ as the incident and scattering wave numbers, respectively, $\hat{k}_\alpha$ and $\hat{k}_\beta$ are unit wave number vectors for *P*- and *S*-waves, and

$$\begin{aligned}&\mathbf{k}_\alpha=\mathbf{K}_T+\gamma_\alpha\hat{\mathbf{e}}_z, \quad \mathbf{k}_\beta=\mathbf{K}_T+\gamma_\beta\hat{\mathbf{e}}_z,\\ &\mathbf{k}_\alpha'=\mathbf{K}_T'\pm\gamma_\alpha'\hat{\mathbf{e}}_z, \quad \mathbf{k}_\beta'=\mathbf{K}_T'\pm\gamma_\beta'\hat{\mathbf{e}}_z,\end{aligned} \tag{17}$$

where the $+$ or $-$ sign depends on whether it is forward or backward scattering, and $\hat{\mathbf{e}}_z$ is the unit vector in the z-direction. The longitudinal coordinate z_0 has been temporarily omitted from these equations.

Equations (13)–(16) give scattered fields of different wave types. They are scattered plane waves with transverse wave number $\mathbf{K}_T'$ generated by the plane incident wave with transverse wave number $\mathbf{K}_T$. The total scattered plane wave is the integration of contributions from all incident plane waves,

$$\mathbf{U}(\mathbf{K}_T',z_0)=\frac{1}{4\pi^2}\int d\mathbf{K}_T\mathbf{U}(\mathbf{K}_T',\mathbf{K}_T,z_0). \tag{18}$$

In principle, Eqs. (7)–(18) provide all equations needed for calculating wave fields $\mathbf{u}_f(\mathbf{x}_T,z_1)$ and $\mathbf{u}_b(\mathbf{x}_T,z_0)$. However, from these equations we can see that scattered waves composed of contributions from all $\mathbf{K}_T'$ which are coupled with all incident $\mathbf{K}_T$. For a general three-dimensional velocity model, both of them are two-dimensional and the $\mathbf{U}(\mathbf{K}_T',\mathbf{K}_T)$ is a four-dimensional matrix. The calculations of these matrix operations are very time consuming. To obtain a highly efficient algorithm, we introduce a small angle approximation to the formulation.

III. SMALL ANGLE APPROXIMATION

Under the small angle approximation, γ_α and γ_α' can be approximated by k_α, and γ_β and γ_β' by k_β. The exchange wave numbers for forward and backward scattered fields can be simplified. For forward scattering

$$\begin{aligned}&\mathbf{k}_\alpha'-\mathbf{k}_\alpha\approx\mathbf{K}_T'-\mathbf{K}_T+0\hat{\mathbf{e}}_z,\\ &\mathbf{k}_\beta'-\mathbf{k}_\alpha\approx\mathbf{K}_T'-\mathbf{K}_T+(k_\beta-k_\alpha)\hat{\mathbf{e}}_z,\\ &\mathbf{k}_\alpha'-\mathbf{k}_\beta\approx\mathbf{K}_T'-\mathbf{K}_T+(k_\alpha-k_\beta)\hat{\mathbf{e}}_z,\\ &\mathbf{k}_\beta'-\mathbf{k}_\beta\approx\mathbf{K}_T'-\mathbf{K}_T+0\hat{\mathbf{e}}_z.\end{aligned} \tag{19}$$

For backward scattering

$$\begin{aligned}&\mathbf{k}_\alpha'-\mathbf{k}_\alpha\approx\mathbf{K}_T'-\mathbf{K}_T-2k_\alpha\hat{\mathbf{e}}_z,\\ &\mathbf{k}_\beta'-\mathbf{k}_\alpha\approx\mathbf{K}_T'-\mathbf{K}_T-(k_\beta+k_\alpha)\hat{\mathbf{e}}_z,\\ &\mathbf{k}_\alpha'-\mathbf{k}_\beta\approx\mathbf{K}_T'-\mathbf{K}_T-(k_\alpha+k_\beta)\hat{\mathbf{e}}_z,\\ &\mathbf{k}_\beta'-\mathbf{k}_\beta\approx\mathbf{K}_T'-\mathbf{K}_T-2k_\beta\hat{\mathbf{e}}_z.\end{aligned} \tag{20}$$

The three-dimensional Fourier transforms of the perturbations $\delta\rho(\mathbf{k})$, $\delta\lambda(\mathbf{k})$ and $\delta\mu(\mathbf{k})$ can also be simplified. Taking the density perturbation for back scattering as an example,

$$\delta\rho(\mathbf{k}_\alpha'-\mathbf{k}_\alpha)=\int_0^{\Delta z}dz e^{i(\gamma_\alpha'+\gamma_\alpha)z}\int\int d\mathbf{x}_T \times\delta\rho(\mathbf{x}_T,z-z_0)e^{-i(\mathbf{K}_T'-\mathbf{K}_T)\cdot\mathbf{x}_T}. \tag{21}$$

If the slab is thin enough, the variation of $\delta\rho(\mathbf{x}_T,z)$ along the z-direction will be small, the integral can be approximated as

$$\delta\rho(\mathbf{k}_\alpha'-\mathbf{k}_\alpha)\approx\Delta z\,\delta\rho(\mathbf{K}_T'-\mathbf{K}_T,z_0)\,\eta_b^{PP}, \tag{22}$$

where

$$\eta_b^{PP}=\frac{1}{i2k_\alpha\Delta z}(e^{i2k_\alpha\Delta z}-1)=\mathrm{sinc}(k_\alpha\Delta z)e^{ik_\alpha\Delta z}, \tag{23}$$

and $\mathrm{sinc}(z)=\sin(z)/z$. In the above equations, the original three-dimensional Fourier transform has been decomposed into a 2D Fourier transform and a 1D Fourier transform. $\delta\rho(\mathbf{K}_T,z_0)$ is a 2D Fourier transform of $\delta\rho(\mathbf{x}_T,z)$ averaged over an interval between z_0 and z_1, η_b^{PP} is the 1D Fourier transform of a boxcar function since the medium variation in z direction has been neglected due to the screen assumption. For simplicity, z_0 is omitted in the following equations. Similarly, for forward scatterings of different wave types we have

$$
\begin{aligned}
&\delta\rho(\mathbf{k}'_\alpha-\mathbf{k}_\alpha)\approx\Delta z\,\delta\rho(\mathbf{K}'_T-\mathbf{K}_T)\,\eta_f^{PP},\\
&\delta\rho(\mathbf{k}'_\beta-\mathbf{k}_\alpha)\approx\Delta z\,\delta\rho(\mathbf{K}'_T-\mathbf{K}_T)\,\eta_f^{PS},\\
&\delta\rho(\mathbf{k}'_\alpha-\mathbf{k}_\beta)\approx\Delta z\,\delta\rho(\mathbf{K}'_T-\mathbf{K}_T)\,\eta_f^{SP},\\
&\delta\rho(\mathbf{k}'_\beta-\mathbf{k}_\beta)\approx\Delta z\,\delta\rho(\mathbf{K}'_T-\mathbf{K}_T)\,\eta_f^{SS},
\end{aligned}
\tag{24}
$$

and for backward scatterings of different wave types

$$
\begin{aligned}
&\delta\rho(\mathbf{k}'_\alpha-\mathbf{k}_\alpha)\approx\Delta z\,\delta\rho(\mathbf{K}'_T-\mathbf{K}_T)\,\eta_b^{PP},\\
&\delta\rho(\mathbf{k}'_\beta-\mathbf{k}_\alpha)\approx\Delta z\,\delta\rho(\mathbf{K}'_T-\mathbf{K}_T)\,\eta_b^{PS},\\
&\delta\rho(\mathbf{k}'_\alpha-\mathbf{k}_\beta)\approx\Delta z\,\delta\rho(\mathbf{K}'_T-\mathbf{K}_T)\,\eta_b^{SP},\\
&\delta\rho(\mathbf{k}'_\beta-\mathbf{k}_\beta)\approx\Delta z\,\delta\rho(\mathbf{K}'_T-\mathbf{K}_T)\,\eta_b^{SS}.
\end{aligned}
\tag{25}
$$

The modulation factors are

$$
\begin{aligned}
&\eta_f^{PP}=1,\\
&\eta_f^{PS}=\mathrm{sinc}[(k_\beta-k_\alpha)\Delta z/2]e^{-i(k_\beta-k_\alpha)\Delta z/2},\\
&\eta_f^{SP}=\eta_f^{*PS},\\
&\eta_f^{SS}=1,
\end{aligned}
\tag{26}
$$

$$
\begin{aligned}
&\eta_b^{PP}=\mathrm{sinc}(k_\alpha\Delta z)e^{ik_\alpha\Delta z},\\
&\eta_b^{PS}=\mathrm{sinc}[(k_\beta+k_\alpha)\Delta z/2]e^{i(k_\beta+k_\alpha)\Delta z/2},\\
&\eta_b^{SP}=\eta_b^{PS},\\
&\eta_b^{SS}=\mathrm{sinc}(k_\beta\Delta z)e^{ik_\beta\Delta z},
\end{aligned}
\tag{27}
$$

where η^* is the complex conjugate of η. Similar expressions can be derived for the elastic constants λ and μ.

Note that under small angle approximation, $(\hat{k}_\alpha\cdot\hat{k}'_\alpha)$, $(\hat{k}_\beta\cdot\hat{k}'_\beta)$, $(\hat{k}_\beta\cdot\hat{k}'_\alpha)$ and $(\hat{k}_\alpha\cdot\hat{k}'_\beta)$ approach $+1$ for forward and -1 for backward scatterings, respectively. Substituting Eqs. (24)–(27) into Eqs. (13)–(16), for forward scatterings we have

$$
\mathbf{U}_f^{PP}(\mathbf{K}'_T,\mathbf{K}_T)=-ik_\alpha\Delta z\hat{k}'_\alpha u_0^P(\mathbf{K}_T)\,\frac{\delta\alpha(\tilde{\mathbf{K}}_T)}{\alpha_0}\,\eta_f^{PP},
\tag{28}
$$

$$
\mathbf{U}_f^{PS}(\mathbf{K}'_T,\mathbf{K}_T)=-ik_\beta\Delta z u_0^P(\mathbf{K}_T)[\hat{k}_\alpha-\hat{k}'_\beta(\hat{k}_\alpha\cdot\hat{k}'_\beta)]\times\left[\frac{\delta\beta(\tilde{\mathbf{K}}_T)}{\beta_0}+\left(\frac{\beta_0}{\alpha_0}-\frac{1}{2}\right)\frac{\delta\mu(\tilde{\mathbf{K}}_T)}{\mu_0}\right]\eta_f^{PS},
\tag{29}
$$

$$
\mathbf{U}_f^{SP}(\mathbf{K}'_T,\mathbf{K}_T)=-ik_\alpha\Delta z(\mathbf{u}_0^S(\mathbf{K}_T)\cdot\hat{k}'_\alpha)\hat{k}'_\alpha\times\left[\frac{\delta\beta(\tilde{\mathbf{K}}_T)}{\beta_0}+\left(\frac{\beta_0}{\alpha_0}-\frac{1}{2}\right)\frac{\delta\mu(\tilde{\mathbf{K}}_T)}{\mu_0}\right]\eta_f^{SP},
\tag{30}
$$

$$
\mathbf{U}_f^{SS}(\mathbf{K}'_T,\mathbf{K}_T)=-ik_\beta\Delta z[\mathbf{u}_0^S(\mathbf{K}_T)-\hat{k}'_\beta(\mathbf{u}_0^S(\mathbf{K}_T)\cdot\hat{k}'_\beta)]\times\frac{\delta\beta(\tilde{\mathbf{K}}_T)}{\beta_0}\,\eta_f^{SS},
\tag{31}
$$

and for backward scatterings, we have

$$
\begin{aligned}
\mathbf{U}_b^{PP}(\mathbf{K}'_T,\mathbf{K}_T)&=-ik_\alpha\Delta z\hat{k}'_\alpha u_0^P(\mathbf{K}_T)\times\left[\frac{\delta\rho(\tilde{\mathbf{K}}_T)}{\rho_0}+\frac{\delta\alpha(\tilde{\mathbf{K}}_T)}{\alpha_0}\right]\eta_b^{PP}\\
&=-ik_\alpha\Delta z\hat{k}'_\alpha u_0^P(\mathbf{K}_T)\,\frac{\delta Z_\alpha(\tilde{\mathbf{K}}_T)}{Z_{\alpha 0}}\,\eta_b^{PP},
\end{aligned}
\tag{32}
$$

$$
\begin{aligned}
\mathbf{U}_b^{PS}(\mathbf{K}'_T,\mathbf{K}_T)&=-ik_\beta\Delta z u_0^P(\mathbf{K}_T)[\hat{k}_\alpha-\hat{k}'_\beta(\hat{k}_\alpha\cdot\hat{k}'_\beta)]\times\left[\frac{\delta\beta(\tilde{\mathbf{K}}_T)}{\beta_0}-\left(\frac{\beta_0}{\alpha_0}+\frac{1}{2}\right)\frac{\delta\mu(\tilde{\mathbf{K}}_T)}{\mu_0}\right]\eta_b^{PS}\\
&=ik_\beta\Delta z u_0^P(\mathbf{K}_T)[\hat{k}_\alpha-\hat{k}'_\beta(\hat{k}_\alpha\cdot\hat{k}'_\beta)]\times\left[\frac{\delta Z_\beta(\tilde{\mathbf{K}}_T)}{Z_{\beta 0}}+\left(\frac{\beta_0}{\alpha_0}-\frac{1}{2}\right)\frac{\delta\mu(\tilde{\mathbf{K}}_T)}{\mu_0}\right]\eta_b^{PS},
\end{aligned}
\tag{33}
$$

$$
\begin{aligned}
\mathbf{U}_b^{SP}(\mathbf{K}'_T,\mathbf{K}_T)&=-ik_\alpha\Delta z(\mathbf{u}_0^S(\mathbf{K}_T)\cdot\hat{k}'_\alpha)\hat{k}'_\alpha\times\left[\frac{\delta\beta(\tilde{\mathbf{K}}_T)}{\beta_0}-\left(\frac{\beta_0}{\alpha_0}+\frac{1}{2}\right)\frac{\delta\mu(\tilde{\mathbf{K}}_T)}{\mu_0}\right]\eta_b^{SP}\\
&=ik_\alpha\Delta z(\mathbf{u}_0^S(\mathbf{K}_T)\cdot\hat{k}'_\alpha)\hat{k}'_\alpha\times\left[\frac{\delta Z_\beta(\tilde{\mathbf{K}}_T)}{Z_{\beta 0}}+\left(\frac{\beta_0}{\alpha_0}-\frac{1}{2}\right)\frac{\delta\mu(\tilde{\mathbf{K}}_T)}{\mu_0}\right]\eta_b^{SP},
\end{aligned}
\tag{34}
$$

$$
\begin{aligned}
\mathbf{U}_b^{SS}(\mathbf{K}'_T,\mathbf{K}_T)&=ik_\beta\Delta z[\mathbf{u}_0^S(\mathbf{K}_T)-\hat{k}'_\beta(\mathbf{u}_0^S(\mathbf{K}_T)\cdot\hat{k}'_\beta)]\times\left[\frac{\delta\rho(\tilde{\mathbf{K}}_T)}{\rho_0}+\frac{\delta\beta(\tilde{\mathbf{K}}_T)}{\beta_0}\right]\eta_b^{SS}\\
&=ik_\beta\Delta z[\mathbf{u}_0^S(\mathbf{K}_T)-\hat{k}'_\beta(\mathbf{u}_0^S(\mathbf{K}_T)\cdot\hat{k}'_\beta)]\times\frac{\delta Z_\beta(\tilde{\mathbf{K}}_T)}{Z_{\beta 0}}\,\eta_b^{SS}.
\end{aligned}
\tag{35}
$$

In Eqs. (28)–(35), $\tilde{\mathbf{K}}_T=\mathbf{K}'_T-\mathbf{K}_T$ is the exchange transverse wave number, $\delta\alpha(\mathbf{K}_T)$ and $\delta\beta(\mathbf{K}_T)$ are transverse spectra of *P*- and *S*-wave velocity perturbations, $\delta Z_\alpha(\mathbf{K}_T)$ and $\delta Z_\beta(\mathbf{K}_T)$ are transverse spectra of *P*- and *S*-wave impedance perturbations, respectively. Equations (28) and (32) show that the forward scattered *P-P* wave is proportional to the *P*-wave velocity perturbation, while the backward scattered *P-P* wave depends on the *P*-wave impedance perturbation, consistent with the scattering theory. A similar situation is true for *S-S* scattering as can be seen from Eqs. (31) and (35). The quantity $(\beta_0/\alpha_0-1/2)$ is usually small, and as can be seen from Eqs. (29) and (30), the forward converted waves $\mathbf{U}_f^{PS}$ and $\mathbf{U}_f^{SP}$ are basically controlled by the *S*-wave velocity perturbation. Similarly, from Eqs. (33) and (34), the backward converted waves $\mathbf{U}_b^{PS}$ and $\mathbf{U}_b^{SP}$ are controlled by *S*-wave impedance perturbation. The forward and backward scattered waves reveal different characteristics of the medium, since they are controlled by different medium parameters.

The total scattered plane wave is the integration of contributions from scattering of all incident plane waves. For example, for *P-P* forward scattering we have

$$\mathbf{U}_f^{PP}(\mathbf{K}_T',z_0)=\frac{1}{4\pi^2}\int d\mathbf{K}_T\mathbf{U}_f^{PP}(\mathbf{K}_T',\mathbf{K}_T,z_0).$$

From Eq. (28) we can see that the above equation is a convolution between the incident wave and medium parameter in the transverse wave number domain. A more efficient calculation is to transfer the wave number domain convolution into a spatial domain multiplication using the fast Fourier transform. Thus

$$\mathbf{U}_f^{PP}(\mathbf{K}_T',z_0)=-ik_\alpha\Delta z\hat{k}_\alpha'\eta_f^{PP}\int\int d\mathbf{x}_f'e^{-i\mathbf{K}_T'\cdot\mathbf{x}_T'}\times u_0^P(\mathbf{x}_T',z_0)\frac{\delta\alpha(\mathbf{x}_T')}{\alpha_0}, \tag{36}$$

where $\delta\alpha(\mathbf{x}_T)$ is $\delta\alpha(\mathbf{x}_T,z)$ averaged over the interval between z_0 and z_1. Similarly, dual-domain formulas for other wave types can be obtained as

$$\mathbf{U}_f^{PS}(\mathbf{K}_T',z_0)=-ik_\beta\Delta z\,\eta_f^{PS}\hat{k}_\beta'\times\left\{\hat{k}_\beta'\times\int\int d\mathbf{x}_T'e^{-i\mathbf{K}_T'\cdot\mathbf{x}_T'}\times\mathbf{u}_0^P(\mathbf{x}_T',z_0)\left[\left(\frac{\beta_0}{\alpha_0}-\frac{1}{2}\right)\frac{\delta\rho(\mathbf{x}_T')}{\rho_0}+2\left(\frac{\beta_0}{\alpha_0}\right)\frac{\delta\beta(\mathbf{x}_T')}{\beta_0}\right]\right\}, \tag{37}$$

$$\mathbf{U}_f^{SP}(\mathbf{K}_T',z_0)=-ik_\alpha\Delta z\,\eta_f^{SP}\hat{k}_\alpha'\left\{\hat{k}_\alpha'\cdot\int\int d\mathbf{x}_T'e^{-i\mathbf{K}_T'\cdot\mathbf{x}_T'}\times\mathbf{u}_0^S(\mathbf{x}_T',z_0)\left[\left(\frac{\beta_0}{\alpha_0}-\frac{1}{2}\right)\frac{\delta\rho(\mathbf{x}_T')}{\rho_0}+2\left(\frac{\beta_0}{\alpha_0}\right)\frac{\delta\beta(\mathbf{x}_T')}{\beta_0}\right]\right\}, \tag{38}$$

$$\mathbf{U}_f^{SS}(\mathbf{K}_T',z_0)=-ik_\beta\Delta z\,\eta_f^{SS}\hat{k}_\beta'\times\left\{\hat{k}_\beta'\int\int d\mathbf{x}_T'\times e^{-i\mathbf{K}_T'\cdot\mathbf{x}_T'}\mathbf{u}_0^S(\mathbf{x}_T',z_0)\frac{\delta\beta(\mathbf{x}_T')}{\beta_0}\right\}, \tag{39}$$

$$\mathbf{U}_b^{PP}(\mathbf{K}_T',z_0)=-ik_\alpha\Delta z\hat{k}_\alpha'\eta_b^{PP}\int\int d\mathbf{x}_T'e^{-i\mathbf{K}_T'\cdot\mathbf{x}_T'}\times u_0^P(\mathbf{x}_T',z_0)\frac{\delta Z_\alpha(\mathbf{x}_T')}{Z_{\alpha0}}, \tag{40}$$

$$\mathbf{U}_b^{PS}(\mathbf{K}_T',z_0)=ik_\beta\Delta z\,\eta_b^{PS}\hat{k}_\beta'\times\left\{\hat{k}_\beta'\times\int\int d\mathbf{x}_T'e^{-i\mathbf{K}_T'\cdot\mathbf{x}_T'}\times\mathbf{u}_0^P(\mathbf{x}_T',z_0)\left[\left(\frac{\beta_0}{\alpha_0}+\frac{1}{2}\right)\frac{\delta\rho(\mathbf{x}_T')}{\rho_0}+2\left(\frac{\beta_0}{\alpha_0}\right)\frac{\delta\beta(\mathbf{x}_T')}{\beta_0}\right]\right\}, \tag{41}$$

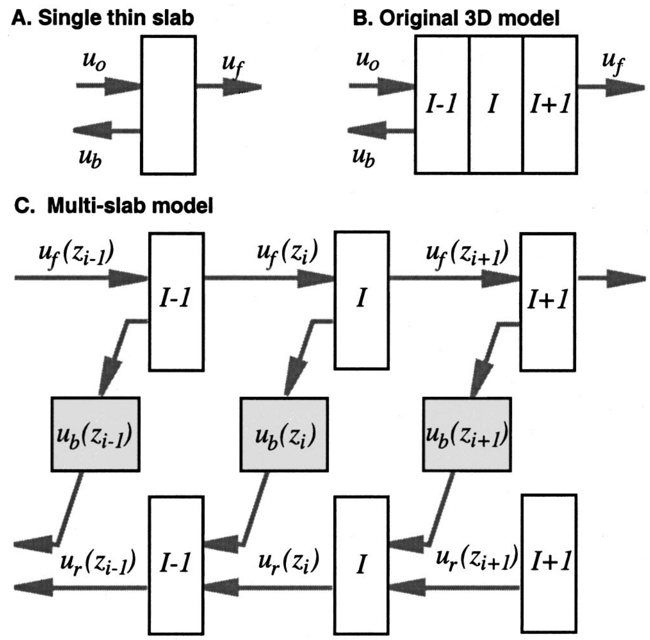

FIG. 2. A sketch of the multiscreen method. For details see text.

$$\mathbf{U}_b^{SP}(\mathbf{K}_T',z_0)=ik_\alpha\Delta z\,\eta_b^{SP}\hat{k}_\alpha'\left\{\hat{k}_\alpha'\cdot\int\int d\mathbf{x}_T'e^{-i\mathbf{K}_T'\cdot\mathbf{x}_T'}\times\mathbf{u}_0^S(\mathbf{x}_T',z_0)\left[\left(\frac{\beta_0}{\alpha_0}+\frac{1}{2}\right)\frac{\delta\rho(\mathbf{x}_T')}{\rho_0}+2\left(\frac{\beta_0}{\alpha_0}\right)\frac{\delta\beta(\mathbf{x}_T')}{\beta_0}\right]\right\}, \tag{42}$$

$$\mathbf{U}_b^{SS}(\mathbf{K}_T',z_0)=ik_\beta\Delta z\,\eta_b^{SS}\hat{k}_\beta'\times\left\{\hat{k}_\beta'\times\int\int d\mathbf{x}_T'e^{-i\mathbf{K}_T'\cdot\mathbf{x}_T'}\times\mathbf{u}_0^S(\mathbf{x}_T',z_0)\frac{\delta Z_\beta(\mathbf{x}_T')}{Z_{\beta0}}\right\}. \tag{43}$$

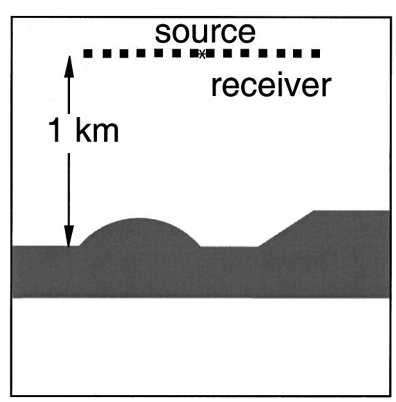

FIG. 3. Two-dimensional model used to compare the results from the screen approximation method and finite-difference method. The model is a 2D profile from the French model (French, 1974). The parameters for the background medium are $V_P=3.6$ km/s, $V_S=2.08$ km/s and $\rho=2.2$ g/cm^3. The intermediate layer has a -20% perturbation for both P- and S-wave velocities.

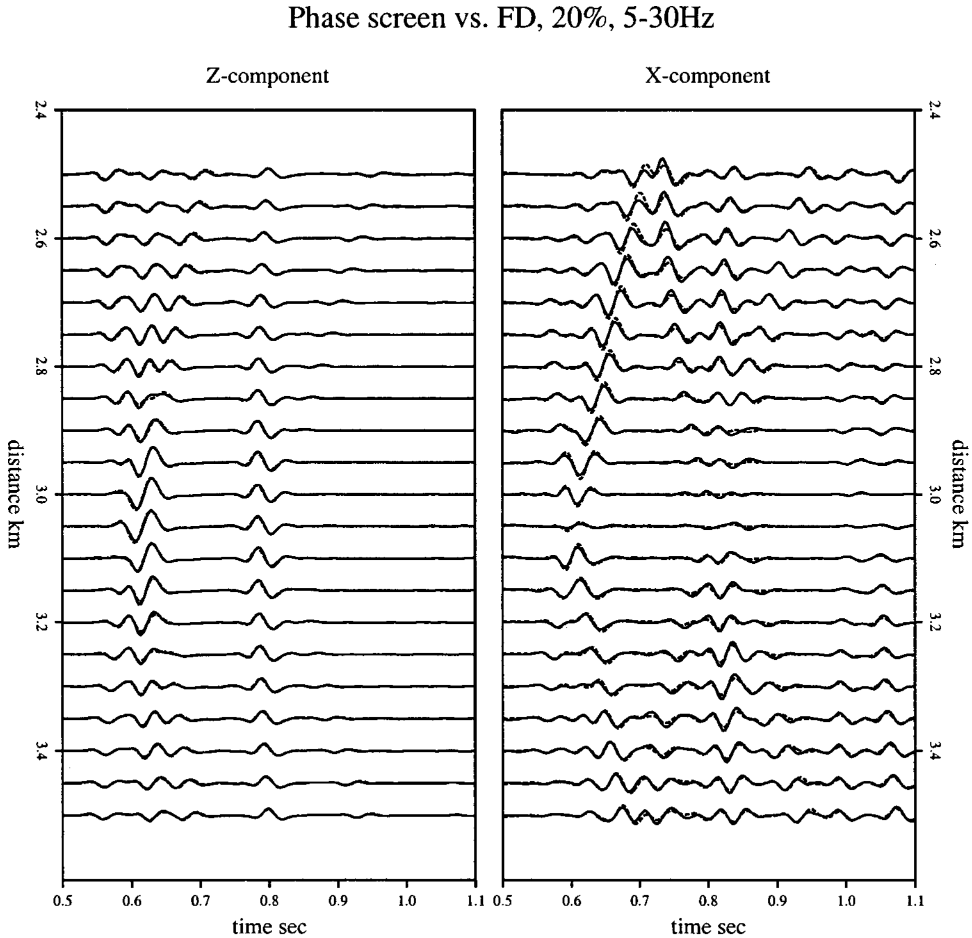

FIG. 4. Comparison of synthetic seismograms calculated by different methods. The solid lines are from the screen method and the dashed lines are from the finite-difference method. The results show general agreement between the two methods in both amplitude and arrival times.

The spatial domain operation of medium-wave interactions are multiplications which are very efficient. The scattered field $\mathbf{U}(\mathbf{K}_T', z)$ from Eqs. (36)–(43) is then substituted into Eqs. (7)–(12) to calculate forward and reflected fields. The propagation of plane waves passing through the homogeneous background medium is conducted in wave number domain by Eqs. (8) and (9). In wave number domain, the propagation operator involves only a phase advance, which is also an efficient operation. Note the difference between Eqs. (13)–(16) and Eqs. (28)–(35). The former involves complicated calculations and the medium-wave interactions are not local, while the later involves simple convolutions in the transverse wave number domain, which results from the small angle approximation and greatly simplifies the calculation.

In summary, the wave propagation through a thin slab is decomposed into a series of highly efficient steps. The model parameters are separated into two parts, the background parameters and the perturbations. The interaction with the perturbations in the spatial domain gives the scattered waves. The propagation through the background medium is in the wave number domain. The calculations in both domains are local and very efficient. The forward and inverse fast Fourier transforms switch the wave field between the two domains.

IV. ITERATIVE PROCEDURE AND NUMERICAL EXAMPLES

Figure 2 is a sketch showing how to calculate the interaction between incident wave and a 3D heterogeneous model with an iterative method. First, the 3D model is divided into a series of thin slabs [Fig. 2(B)]. The Ith slab is between z_i and z_{i+1}. The last section provides us with the formulas for calculating the interaction between the incident wave and a single thin slab [Fig. 2(A)]. With these equations we can calculate the transmitted field $u_f(z_{i+1})$ and the backscattered field $u_b(z_i)$ from the incident wave $u_f(z_i)$. The transmitted field is used as the input for the next slab and in this way the forward propagated field in the entire model can be obtained. The backscattered field are stored temporarily. After finishing the forward propagation, the backscattered fields are retrieved and once again propagated using the one-way propagator. The reflected fields $u_r(z)$ in the entire model are calculated [Fig. 2(C)]. In this way, all the multiple forward scatterings and single backscatterings (MFSB) can be taken into account.

Numerical simulations are conducted to test the accuracy and efficiency of this method. The model is a 2D cut from the French model (French, 1974). Figure 3 shows the velocity structure of this model. The parameters of the background medium are $V_P = 3.6$ km/s, $V_S = 2.08$ km/s, and $\rho = 2.2$ g/cm^3. The intermediate layer has a -20% perturbation for both P- and S-wave velocities. The P-wave source and receivers are located 1 km above the upper interface. With this source–receiver configuration, the observed signals are basically reflections from the structure. The synthetic seismograms are calculated using the elastic complex-screen method presented in this study and a finite-difference method. The later is a fourth order elastic wave finite-difference code (Xie and Yao, 1988; Xie and Lay, 1994). Free surface effects and primary arrivals have been properly removed from these results. The synthetic seismograms are compared in Fig. 4. Solid lines are from the complex-screen method and the dashed lines are from the finite-difference method. For the *z*-component, there are mainly *P*-waves. The waves arriving between 0.5 and 0.7 s are *P-P* reflections from different parts of the upper interface. Several arrivals can be identified. The second group of waves is relatively simple. They are *P*-to-*P* reflections from the lower plane interface. Due to the complexity of the upper interface, both *P-P* and *P-S* reflections from this interface are rather complicated. They are composed of reflections from the flat and curved sections, and diffractions from the sharp corner. The later is a challenge for ray-based methods. The transverse components of the synthetics are composed of *P-S* reflections from both interfaces, as well as some *P*-waves. Generally speaking, the agreement between the two methods is very good.

V. CONCLUSIONS

The elastic complex-screen method is based on the one-way wave equation, local Born approximation and small angle approximation. It provides an efficient way for calculating both forward and backward scattered waves. This method calculates both forward propagating waves and primary reflections for complicated models. As an example, synthetic seismograms for a 2D elastic model are calculated with this method. The results are compared with those of a finite-difference method. For small to medium scattering angles and medium velocity contrast, the method is well in agreement with the finite-difference method. For wide scattering angles, there are errors in synthetic seismograms. Further investigations show that the errors result from the small angle approximation to the scattering radiation pattern (Wu and Wu, 1998) and phase delay under wide angle and large velocity perturbation (Ristow and Ruhl, 1994; Xie and Wu, 1998). Wide angle accuracy should be further improved in future studies.

ACKNOWLEDGMENTS

This research is supported by the Office of Naval Research under Grant No. N00014-95-1-0093. The facility support from the W. M. Keck Foundation is also acknowledged. Contribution No. 437 of the IGPP, University of California, Santa Cruz.

Aki, K., and Richards, P. G. (**1980**). *Quantitative Seismology: Theory and Methods*, Vol. 1 (W. H. Freeman, New York), pp. 9–36.

Beydoun, W. B., and Mendes, M. (**1989**). ''Elastic ray-Born l_2-migration/inversion,'' Geophys. J. Int. **97**, 151–160.

Červený, V. (**1981**). ''Seismic wave fields in structurally complicated media (Ray and Gaussian beam approaches),'' Lecture Notes, Rijksuniversiteit Utrecht, Vening-Meinesz Laboratory, Utrecht.

Červený, V., and Klimeš, L. (**1984**). ''Synthetic body wave seismograms for three-dimensional laterally varying media,'' Geophys. J. Int. **79**, 119–133.

Chapman, C. H. (**1985**). ''Ray theory and its extensions: WKBJ and Maslov seismograms,'' J. Geophys. **58**, 27–43.

Coates, R. T., and Chapman, C. H. (**1990**). ''Ray perturbation theory and the Born approximation,'' Geophys. J. Int. **100**, 379–392.

Coates, R. T., and Chapman, C. H. (**1991**). ''Generalized Born scattering of elastic waves in 3-D media,'' Geophys. J. Int. **107**, 231–263.

Fisk, M. D., and McCartor, G. D. (**1991**). ''The phase screen method for vector elastic waves,'' J. Geophys. Res. **96**, 5985–6010.

Flatté, S. M., and Tappert, F. D. (**1975**). ''Calculation of the effect of internal waves on oceanic sound transmission,'' J. Acoust. Soc. Am. **58**, 1151–1159.

French, W. S. (**1974**). ''Two-dimensional and three-dimensional migration of model-experiment reflection profiles,'' Geophysics **39**, 265–277.

Gubernatis, J. E., Domany, E., Krumhansl, J. A., and Huberman, M. (**1977**). ''The Born approximation in the theory of the scattering of elastic waves by flaws,'' J. Appl. Phys. **48**, 2812–2819.

Huang, L. J., Fehler, M. C., and Wu, R. S. (**1999**). ''Extended local Born Fourier migration method,'' Geophysics **64**, 1524–1534.

Ristow, D., and Ruhl, T. (**1994**). ''Fourier finite-difference migration,'' Geophysics **59**, 1882–1893.

Stoffa, P. L., Fokkema, J. T., Freire, R. M. D., and Kessinger, W. P. (**1990**). ''Split-step Fourier migration,'' Geophysics **55**, 410–421.

Tappert, F. D. (**1977**). ''The parabolic equation method,'' in *Wave Propagation and Underwater Acoustics*, edited by Keller and Papadakis (Springer, New York), pp. 224–287.

Thomson, D. J., and Chapman, N. R. (**1983**). ''A wide-angle split-step algorithm for the parabolic equation,'' J. Acoust. Soc. Am. **74**, 1848–1854.

Wild, J., and Hudson, J. A. (**1998**). ''A geometrical approach to the elastic complex screen,'' J. Geophys. Res. **103**, 707–726.

Wu, R. S. (**1994**). ''Wide-angle elastic wave one-way propagation in heterogeneous media and an elastic wave complex-screen method,'' J. Geophys. Res. **99**, 751–766.

Wu, R. S. (**1996**). ''Synthetic seismograms in heterogeneous media by one-return approximation,'' Pure Appl. Geophys. **148**, 155–173.

Wu, R. S., and Aki, K. (**1985**). ''Scattering characteristics of waves by an elastic heterogeneity,'' Geophysics **50**, 582–595.

Wu, R. S., and Huang, L. J. (**1995**). ''Reflected wave modeling in heterogeneous acoustic media using the De Wolf approximation,'' in *Mathematical Methods in Geophysical Imaging III*, SPIE Proceedings Series **2571**, 176–193.

Wu, R. S., and Xie, X. B. (**1994**). ''Multi-screen backpropagator for fast 3D elastic prestack migration,'' in *Mathematical Methods in Geophysical Imaging II*, SPIE Proceedings Series **2301**, 181–193.

Wu, X., and Wu, R. S. (**1998**). ''An improvement to complex screen method for modeling elastic wave reflections,'' Expanded abstracts, SEG 68th Annual Meeting, pp. 1941–1944.

Xie, X. B., and Lay, T. (**1994**). ''The excitation of Lg waves by explosions: A finite-difference investigation,'' Bull. Seismol. Soc. Am. **84**, 324–342.

Xie, X. B., and Wu, R. S. (**1996**). ''3D elastic wave modeling using the complex screen method,'' Expanded abstracts, SEG 66th Annual Meeting, pp. 1247–1250.

Xie, X. B., and Wu, R. S. (**1998**). ''Improve the wide angle accuracy of screen method under large contrast,'' Expanded abstracts, SEG 68th Annual Meeting, pp. 1811–1814.

Xie, X. B., and Yao, Z. X. (**1988**). ''*P-SV* wave responses for a point source in two-dimensional heterogeneous media, finite-difference method,'' Chinese J. Geophys. **31**, 473–493.